

Core percolation: a new geometric phase transition in random graphs

M. Bauer and O. Golinelli,

*email: {bauer, golinelli}@spht.saclay.cea.fr
 Service de Physique Théorique, Cea Saclay
 91191 Gif-sur-Yvette, France*

January 31, 2001
 Preprint T01/017 ; arXiv:cond-mat/0102011

Abstract

We study both numerically and analytically what happens to a random graph of average connectivity α when its leaves and their neighbors are removed iteratively up to the point when no leaf remains. The remnant is made of isolated vertices plus an induced subgraph we call *the core*. In the thermodynamic limit of an infinite random graph, we compute analytically the dynamics of leaf removal, the number of isolated vertices and the number of vertices and edges in the core. We show that a second order phase transition occurs at $\alpha = e = 2.718\dots$: below the transition, the core is small but above the transition, it occupies a finite fraction of the initial graph. The finite size scaling properties are then studied numerically in detail in the critical region, and we propose a consistent set of critical exponents. This clarifies several aspects in some optimization problems and spectral properties on the adjacency matrix of random graphs.

1 Introduction

What remains of a graph when leaves are iteratively removed until none remains ? The answer depends on what is meant by leaves.

In the most standard acceptation, a leaf is a vertex with exactly one neighbor, and leaf removal deletes this vertex and the adjacent edge. Then, in the context of large random graphs where the connectivity α (the average number of neighbors of a vertex) is kept fixed and the number of vertices $N \rightarrow \infty$, the answer is well known and interesting. When $\alpha < 1$, the remnant after leaf removal is made of $O(N)$ isolated vertices, plus a subgraph a size $o(N)$ without leaves. When $\alpha > 1$, the remnant still contains $O(N)$ isolated points, but the rest is a subgraph of size $O(N)$, which is dominated by a single connected component. In fact, this is just the standard percolation at $\alpha = 1$, discovered and studied in great details by Erdős and Renyi [1]. Indeed, a large random graph of average connectivity $\alpha < 1$ consists of a forest (union of trees) plus a finite number of connected components with one closed loop. Obviously, each tree shrinks to a single isolated point after leaf removal. However, at $\alpha = 1$ the percolation transition occurs and when $\alpha > 1$, a random graph consists of a forest plus a finite number of components with one closed

loop, plus a “giant” connected component containing a finite fraction of the vertices and an extensive number of loops. No loop is destroyed by leaf removal so that the giant component leads to a macroscopic connected remnant after leaf removal. The percolation transition has been studied extensively and many fine details of its structure have been computed (see e.g Ref. [2]).

Of course, one could also consider the removal of more complicated patterns. The next example in complexity is to remove at each step not only the leaf but also its neighbor (and consequently all adjacent edges). To avoid cumbersome circumlocutions, in the rest of this paper, we call *leaf* the pair “standard leaf + its neighbor”. Now leaf removal deletes two vertices (a vertex with a single neighbor and this neighbor) and all the edges adjacent to one or both vertices. It is quite natural to study the removal of these patterns because it has a number of applications to graph theory: several numerical characteristics of a graph behave nicely under leaf removal. One such characteristic, of interest in physics, is the multiplicity of the eigenvalue 0 in the adjacency matrix of the graph. Others are the minimal size of a vertex cover and the maximal size of an edge disjoint subset, questions which are related to various combinatorial optimization problems.

With this definition, we shall elucidate in this paper the

structure of the remnant after iterated leaf removal when the graph is a large random graph of finite connectivity α . We show that for $\alpha < e = 2.718\dots$, the residue consists of $i(\alpha)N + O(1)$ isolated points and an induced subgraph of size $O(1)$ without leaves or isolated points. A second order phase transition occurs at $\alpha = e$. For $\alpha > e$, the residue consists of $i(\alpha)N + O(1)$ isolated points, and a subgraph without leaves or isolated points containing $c(\alpha)N + O(1)$ vertices linked by $l(\alpha)N + O(1)$ edges. We shall argue that this graph is made of a giant connected “core” component plus a finite number of small connected components involving a total of $o(N)$ vertices. This points to a new percolation transition in the random graph model.

The fact that some properties of random graphs are singular at $\alpha = e$ had been observed before in an analytical context (see Ref. [3] for combinatorial optimization problems, and Ref. [4] for localization problems) and in a numerical context (see Ref. [5] where an anomaly in the spectrum of random adjacency matrices close to the eigenvalue 0 was observed).

The paper is organized as follows. The general definitions have been regrouped in section 2. They are standard and should be used only for reference.

In section 3 we define leaf removal, leaf removal processes obtained by iteration of leaf removals and the “core” for an arbitrary graph.

Section 4 presents our main results for large random graphs. The analytical formulæ for $i(\alpha)$, $c(\alpha)$ and $l(\alpha)$ are given.

In section 5, these formulæ are checked against Monte-Carlo simulations of leaf removal processes, which we also use for the finite size scaling analysis in the critical region. This leads us to the definition and numerical evaluation of many new critical exponents.

In section 6, we give two applications of our results on core percolation. We show in particular in section 6.1 that for any α the core of a random graph only carries a small number of 0 eigenvalues of the adjacency matrix and that the emergence of the core has a direct impact on the localized and delocalized eigenvectors of the adjacency matrix with eigenvalue 0. In section 6.2, we show that for $\alpha < e$, the problem of finding minimal vertex covers or maximal edge disjoint subsets can be handled very simply in polynomial time (in fact, in linear time once the graph is encoded in a suitable form). These problems are believed to be NP-hard for general graphs, and the same should be true on the core of a random graph for $\alpha > e$.

2 General definitions

We start with a few standard definitions. This section should be used only for reference.

Graph: A graph (also called a *simple graph* in the mathematical literature) G is a pair consisting of a set

V called the set of vertices of G and a set E called the set of edges of G , whose elements are pairs of distinct elements of V . If $\{v, w\}$ is an edge, the vertices v and w are called *adjacent* or *neighbors*. They are the extremities of the edge $\{v, w\}$. Note that there is at most one edge between two vertices, and that there is no edge connecting a vertex with itself: the word *simple* above refers to these two restrictions.

Adjacency matrix: The adjacency matrix of a graph G is a square matrix $M_{v,w}$ indexed by vertices of G and such that $M_{v,w} = 1$ if $\{v, w\}$ is an edge of G and 0 otherwise. Note that M is a symmetric 0 – 1 matrix with zeroes on the diagonal. Conversely, any such matrix is the adjacency matrix of a graph. We denote by $Z(G)$ the dimension of the kernel (that is, the subspace of eigenvectors with eigenvalue 0) of the adjacency matrix of G .

Induced subgraph: If $V' \subset V$, the graph with vertex set V' and edge set E' those edges in E with both extremities in V' is called the subgraph of G induced by V' .

Random graph in the microcanonical ensemble: If $V = \{1, \dots, N\}$, there are $\binom{N(N-1)/2}{L}$ graphs with vertex set V and L edges (making a total of $2^{N(N-1)/2}$ graphs with vertex set V). Saying that all $\binom{N(N-1)/2}{L}$ are equiprobable turns the set of graphs on N vertices and L edges into a probability space whose elements we call *random graphs in the microcanonical ensemble*. This is the ensemble we use below for numerical simulations.

Random graph in the canonical ensemble: Given a number $p \in [0, 1]$, we introduce $\frac{N(N-1)}{2}$ independent random variables $\varepsilon_{i,j}$, $1 \leq i < j \leq N$, each taking value 1 with probability p and 0 with probability $1 - p$. Saying that $\{i, j\}$ is an edge of G if and only if $\varepsilon_{i,j} = 1$ turns the set of all $2^{N(N-1)/2}$ graphs with vertex set V into a probability space whose elements we call *random graphs in the canonical ensemble*. This is the ensemble we use below for analytical computations.

Connectivity, α : In the sequel, we are interested in the large N limit with a finite limit α for $\frac{2L}{N}$ (microcanonical ensemble) or for $p(N-1)$ (canonical ensemble). The parameter α is the average connectivity, the average number of neighbors of a given vertex in the random graph.

If $N(p(1-p))^{1/2} \rightarrow \infty$ and $L \sim p \frac{N(N-1)}{2}$, the thermodynamic properties of a $G(N, L)$ in the microcanonical ensemble and of a $G(N, p)$ in the canonical ensemble are the same. This is in particular true if $pN = \alpha$ is kept fixed as $N \rightarrow \infty$.

3 Leaf removal process and the core of a graph

Our aim is to define, for any (finite) graph G , a remarkable subgraph which we call the *core* of G . It is obtained by *leaf removal*, an operation that we define now.

Leaf: A leaf of a graph G is a couple of vertices (v, w) such that $\{v, w\}$ is an edge of G and w belongs to no other edge of G . Note that this is not the most standard definition and that (v, w) and (w, v) are both leaves if and only if $\{v, w\}$ is a connected component of G .

Bunch of leaves: A bunch of leaves is a maximal family of leaves with the same first vertex. The leaves of a graph can be grouped into bunches of leaves in an unique way.

Leaf removal: If (v, w) is a leaf of G , and G' the subgraph of G induced by $V \setminus \{v, w\}$, we say that G' is obtained from G by leaf removal of (v, w) . In other words, G' is obtained from G by removing vertices v and w , the edge $\{v, w\}$ and all other edges touching v . Note that this operation can destroy other leaves of G and also create new leaves.

Step by step leaf removal process: Start from a graph G . If G has no leaves, stop. Else, choose a leaf (v, w) and remove it, leading to a graph G' . If G' has no leaves, stop. Else, choose a leaf (v', w') and remove it. This operation is iterated until no leaf remains.

History: A sequence $G, (v, w), G', (v', w'), \dots$ associated to a step by step leaf removal process is called an history.

Isolated points, I ; Core of a graph, C : The last term in an history starting from G is a graph which splits into a collection of isolated points I , and an induced subgraph C of G without leaves or isolated points which we call the core of G . We denote the number of points in the core by N_c and the number of edges in the core by L_c .

For this definition to make sense, one has to show that the core is well defined, that is, does not depend on the choice of history. In fact, we shall show by induction on the number N of vertices of G that the property

$\mathcal{P}_N \equiv$ “the number of isolated points $|I|$ after leaf removal and the core C of a graph G on N vertices do not depend on the history”

holds for any $N \geq 0$.

To start the induction, if G has 0 or 1 vertex, there is no leaf hence there is only one history, so \mathcal{P}_0 and \mathcal{P}_1 are true. Suppose now that $\mathcal{P}_0, \dots, \mathcal{P}_{N-1}$ are proved and take a graph G on $N \geq 2$ vertices. We distinguish several cases:

- 1 If G has no leaf, there is only one history so \mathcal{P}_N is true for G .
- 2 If G has exactly one leaf, all histories start with the same first leaf removal, lead to the same G' for which \mathcal{P}_{N-2} is true by the induction hypothesis, so \mathcal{P}_N is true for G .
- 3 If G has at least two leaves, we compare two histories:

$$\begin{aligned} \mathcal{H}_1 &= G, (v_1, w_1), G'_1, \dots \quad \text{and} \\ \mathcal{H}_2 &= G, (v_2, w_2), G'_2, \dots \end{aligned}$$

3a If $\{v_1, w_1\} = \{v_2, w_2\}$, $G'_1 = G'_2$ to which the induction hypothesis \mathcal{P}_{N-2} applies, so that $C_1 = C_2$ and $|I_1| = |I_2|$.

3b If $v_1 = v_2$ but $w_1 \neq w_2$ (the two leaves are distinct but belong to the same bunch, this can happen only if $N \geq 3$), then G'_1 has w_2 as an isolated point, G'_2 has w_1 as an isolated point, but $G'_1/\{w_2\} = G'_2/\{w_1\} = G''$, say. Further leaf removals can take place only on G'' , to which the induction hypothesis \mathcal{P}_{N-3} applies, so again, $C_1 = C_2$ and $|I_1| = |I_2|$.

3c Suppose that (v_1, w_1) and (v_2, w_2) do not belong to the same bunch. This can happen only if $N \geq 4$. Then (v_1, w_1) is a leaf of G'_2 and (v_2, w_2) is a leaf of G'_1 . The graph obtained from G'_2 by leaf removal of (v_1, w_1) and the graph obtained from G'_1 by leaf removal of (v_2, w_2) are the same, because they are both equal to G'' , the subgraph of G induced by $V \setminus \{v_1, w_1, v_2, w_2\}$. Take a history \mathcal{H}'' for G'' . It can be completed to give two histories for G , $\mathcal{H}_1'' = G, (v_1, w_1), G'_1, (v_2, w_2), \mathcal{H}''$ and $\mathcal{H}_2'' = G, (v_2, w_2), G'_2, (v_1, w_1), \mathcal{H}''$. The induction hypothesis \mathcal{P}_{N-2} applies to G'_1 so \mathcal{H}_1'' and \mathcal{H}_1 have to end with the same core and the same number of isolated points. The same is true for \mathcal{H}_2'' and \mathcal{H}_2 because the induction hypothesis applies \mathcal{P}_{N-2} to G'_2 , and also for \mathcal{H}_1'' and \mathcal{H}_2'' because the induction hypothesis \mathcal{P}_{N-4} applies to G'' . By transitivity, \mathcal{H}_1 and \mathcal{H}_2 end with the same core and the same number of isolated points: $C_1 = C_2$ and $|I_1| = |I_2|$.

All possibilities have been examined, hence whatever the number of leaves of G , \mathcal{P}_N is true for G . This completes the induction step.

Global leaf removal process: Start from a graph G . If it has no leaves, stop. Else select one leaf in every bunch of leaves. Remove from the vertex set V both extremities of all the selected leaves, and define $V^{(1)}$ to be the set of remaining vertices. Let $G^{(1)}$ be the subgraph of G induced by $V^{(1)}$. Note that the leaves of $G^{(1)}$ (if any) are not leaves of G . In this operation, the vertices belonging to a bunch of G that were not selected, become isolated points of $G^{(1)}$. They remain isolated for the rest of the process. Iterate the procedure and define $G^{(2)}, G^{(3)}, \dots$ until a graph without leaves is obtained.

The argument in step **3c** says that leaf removals that take place in distinct bunches of a graph commute. It implies that the global leaf removal process leads to same core and number of isolated points as any step by step leaf removal process.

While the global leaf removal process is convenient for analytical computations, the step by step leaf removal process is easier to implement on the computer.

4 Core percolation: infinite N results

The global leaf removal process allows to compute the most salient characteristics of the leaf removal process, the functions $i(\alpha)$, $c(\alpha)$ and $l(\alpha)$. Remember that by definition, the number of isolated points after leaf removal is $Ni(\alpha) + o(N)$, the number of vertices in the core is $N_c = Nc(\alpha) + o(N)$, and the number of edges in the core is $L_c = Nl(\alpha) + o(N)$. The clue is an enumeration of all the configurations on the random graph that contribute extensively to the fundamental events in the global leaf removal process at step n (which goes from $G^{(n-1)}$ to $G^{(n)}$): emergence of a new isolated point, removal of a point, removal of an edge. This enumeration is possible because the finite configurations of vertices and edges in the random graph with extensive multiplicity are tree-like. This implies that the problem has a recursive structure. One has to be rather careful to avoid double counting and omissions; the examination of all cases is very tedious so we omit the details. The results are as follows.

Let $e_n(\alpha)$ be the sequence of iterated exponentials, defined by

$$e_{-1} = 0 \quad \text{and} \quad e_n = e^{-\alpha e_{n-1}} \quad \text{for} \quad n \geq 0. \quad (1)$$

There is an explicit formula for extensive contribution to the average number $Ni_n(\alpha)$ of isolated vertices, $Nc_n(\alpha)$ of non isolated vertices and $Nl_n(\alpha)$ of edges in $G^{(n)}$, namely

$$\begin{aligned} i_n(\alpha) &= e_{2n+1} + e_{2n} + \alpha e_{2n} e_{2n-1} - 1, \\ c_n(\alpha) &= e_{2n} - e_{2n+1} - \alpha e_{2n} e_{2n-1} + \alpha e_{2n-1}^2, \\ l_n(\alpha) &= \frac{\alpha}{2}(e_{2n} - e_{2n-1})^2. \end{aligned} \quad (2)$$

Now comes the crucial fact: when $\alpha \leq e$, the sequence $e_n(\alpha)$ converges to $W(\alpha)/\alpha$, where $W(\alpha)$ is the Lambert function, defined for $\alpha \geq 0$ as the unique real solution of the equation $We^W = \alpha$. The function $W(\alpha)$ is analytic for $\alpha \geq 0$. When $\alpha > e$, $W(\alpha)/\alpha$ remains a fixed point of the iteration Eq. (1) but it is unstable: the sequence $\{e_n\}$ is oscillating. However the even subsequence e_{2n} and odd subsequences e_{2n+1} are still convergent. The even limit is strictly larger than the odd limit. We define the functions $A(\alpha)$ and $B(\alpha)$ for $\alpha \geq 0$ by

$$\lim_{n \rightarrow \infty} e_{2n} = \frac{B}{\alpha} \quad \text{and} \quad \lim_{n \rightarrow \infty} e_{2n+1} = \frac{A}{\alpha}.$$

Then (A, B) solve the system

$$Ae^B = \alpha, \quad Be^A = \alpha. \quad (3)$$

For $\alpha \leq e$, the unique solution is $A = B = W$. For $\alpha > e$, the previous solution becomes unstable and (A, B) is the solution of Eq. (3) selected by the rule $A < W < B$. This is summarized on Fig. 1.

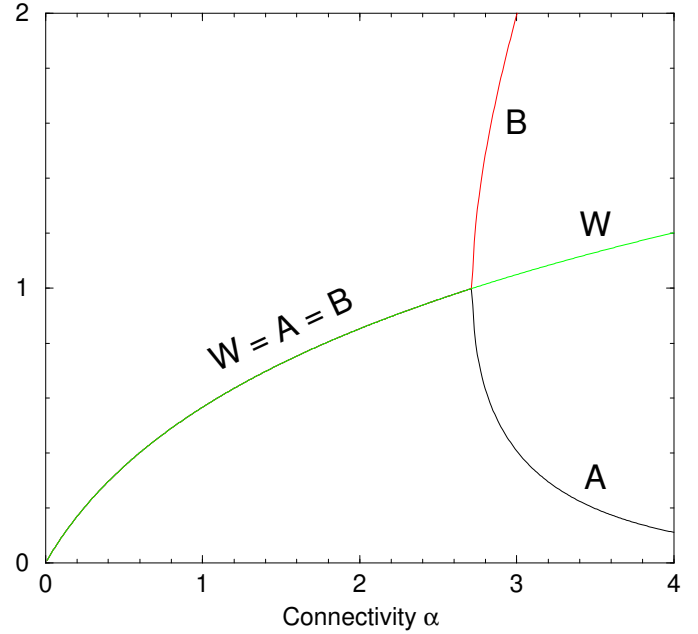


Figure 1: The special functions $W(\alpha)$, $A(\alpha)$ and $B(\alpha)$, which coincide for $\alpha \leq e$.

Taking the limit in Eq. (2) leads to

$$\begin{aligned} i(\alpha) &= \frac{A + B + AB}{\alpha} - 1, \\ c(\alpha) &= \frac{(B - A)(1 - A)}{\alpha}, \\ l(\alpha) &= \frac{(B - A)^2}{2\alpha}. \end{aligned} \quad (4)$$

For $\alpha \leq e$, $c(\alpha) = l(\alpha) = 0$, and the core indeed has a size $o(N)$. On the other hand, the core occupies a finite fraction $c(\alpha)$ of the vertices for $\alpha > e$. The behavior of Eq (1) is responsible of this new geometric transition, core percolation, at $\alpha = e$. As $c(\alpha)$ and $l(\alpha) \rightarrow 0$ when $\alpha \rightarrow e^+$, these functions are continuous but their derivatives are not: the transition is of second order.

The fact that the core of a graph is an induced subgraph of the original graph allows to give a physicist argument for the uniqueness of the giant component in the core. Fix $\alpha > e$. If the core of the random graph contains two or more large connected components, there was no edge with extremities in two components in the original graph. But as the total size of the large connected components is of order N , the absence of such an edge is extremely unlikely.

Writing $\alpha = e(1 + \varepsilon)$, for small negative ε ,

$$A(\alpha) = B(\alpha) = 1 + \frac{1}{2}\varepsilon - \frac{3}{16}\varepsilon^2 + \frac{19}{192}\varepsilon^3 - \frac{185}{3072}\varepsilon^4 + \frac{2437}{61440}\varepsilon^5 + O(\varepsilon^6)$$

while for small positive ε ,

$$A(\alpha) = 1 - 6^{1/2}\varepsilon^{1/2} + 2\varepsilon - \frac{6^{1/2}}{20}\varepsilon^{3/2} - \frac{3}{5}\varepsilon^2 + O(\varepsilon^{3/2}),$$

$$B(\alpha) = 1 + 6^{1/2}\varepsilon^{1/2} + 2\varepsilon + \frac{6^{1/2}}{20}\varepsilon^{3/2} - \frac{3}{5}\varepsilon^2 + O(\varepsilon^{3/2}).$$

For $i(\alpha)$, this implies that there is a jump only in the second derivative of at the transition, with

$$i(\alpha) = \frac{3-e}{e} - \frac{1}{e}\varepsilon + \begin{cases} \frac{1}{2e}\varepsilon^2 + O(\varepsilon^3) & \text{for } \varepsilon < 0 \\ \frac{2}{e}\varepsilon^2 + O(\varepsilon^3) & \text{for } \varepsilon > 0 \end{cases}$$

while $c(\alpha)$ and $l(\alpha)$ have a jump in the first derivative at the transition, with

$$c(\alpha) = \begin{cases} 0 & \text{for } \varepsilon < 0 \\ \frac{12}{e}\varepsilon - \frac{4(6)^{1/2}}{e}\varepsilon^{3/2} - \frac{54}{5e}\varepsilon^2 + O(\varepsilon^{5/2}) & \text{for } \varepsilon > 0 \end{cases}$$

and

$$l(\alpha) = \begin{cases} 0 & \text{for } \varepsilon < 0 \\ \frac{12}{e}\varepsilon - \frac{54}{5e}\varepsilon^2 + O(\varepsilon^3) & \text{for } \varepsilon > 0. \end{cases}$$

The expansion for l contains only integral powers of ε , and this may be related to the fact (see section 5) that the finite size corrections for the number of edges in the core L_c are slightly nicer than the ones for the number of vertices in the core N_c . The average connectivity of the core is

$$\alpha_{eff} = \frac{2l(\alpha)}{c(\alpha)} = \frac{B-A}{1-A} = 2 + \frac{2(6)^{1/2}}{3}\varepsilon^{1/2} + \frac{4}{3}\varepsilon + O(\varepsilon^{3/2})$$

for $\varepsilon > 0$, which implies that giant core component should look like a large loop for α close to e^+ . The exponent $1/2$ in the first correction makes such a property quite difficult to see numerically at large but finite N .

In the random graph model, the vertices do not live in any ambient space, and the notion of correlation length is ambiguous. This problem will reappear in the finite size scaling analysis of the next section. However, the emergence of the core is very reminiscent of critical phenomena in physics. In particular, the critical slowing down is observable during the global leaf removal process. Indeed, the speed of convergence of the iterated exponential sequence can be computed. One finds that for $\alpha \neq e$, the convergence is exponential: if the “convergence rate” $\xi^{-1}(\alpha)$ is defined by the formula

$$\xi^{-1} = \frac{A+B}{2} - \log \alpha,$$

one checks that

$$\begin{aligned} e_n - \frac{W}{\alpha} &\sim (-)^n w e^{-n/\xi} & \text{for } \alpha < e, \\ e_{2n+1} - \frac{A}{\alpha} &\sim -a e^{-(2n+1)/\xi} & \text{for } \alpha > e, \\ e_{2n} - \frac{B}{\alpha} &\sim b e^{-2n/\xi} & \text{for } \alpha > e, \end{aligned}$$

where $a(\alpha)$, $w(\alpha)$ and $b(\alpha)$ are positive functions (they coincide for $\alpha < e$ and $be^{-B/2} = ae^{-A/2}$). When $\alpha \rightarrow e^-$, $\xi \sim \frac{2e}{e-\alpha}$, and when $\alpha \rightarrow e^+$, $\xi \sim \frac{e}{\alpha-e}$.

At $\alpha = e$, the convergence is algebraic, and

$$\begin{aligned} e \left(e_n - \frac{1}{e} \right) &= \\ (-)^n \frac{6^{1/2}}{n^{1/2}} + \frac{3}{2n} + (-)^{n+1} \frac{21(6)^{1/2}}{80} \frac{\log n}{n^{3/2}} + O\left(\frac{1}{n^{3/2}}\right). \end{aligned}$$

This leads to the asymptotics at $\alpha = e$:

$$\begin{aligned} i_n &= \frac{3-e}{e} + O\left(\frac{1}{n^{3/2}}\right), \\ c_n &= \frac{6}{en} \left(1 - \frac{3^{1/2}}{4n^{1/2}} - \frac{21 \log n}{80n} + O\left(\frac{1}{n}\right) \right), \\ l_n &= \frac{6}{en} \left(1 - \frac{21 \log n}{80n} + O\left(\frac{1}{n}\right) \right). \end{aligned}$$

The first correction for c_n is more important than the one for l_n . Moreover the logarithms at $\alpha = e$ lead to suspect that the finite size analysis of the next section might also be complicated by logarithms.

5 Numerical studies of the core percolation

The analytical computations above have enabled us to locate a phase transition at $\alpha = e$, but they give little information concerning the critical region and do not exhaust all the critical exponents. To study these questions, we made an extensive numerical analysis of the core using Monte-Carlo simulations. At the first step this can also be used to check the previous analytical results. But let us start with the numerical algorithm.

5.1 Monte-Carlo algorithm

Our Monte-Carlo simulations consist in generating lots of random graphs, removing leaves step by step, and studying the remaining cores and isolated points. More precisely, for a given set of parameters (N, α) , we generated random graphs in the *microcanonical* ensemble, with N vertices and $L = N\alpha/2$ edges (L is rounded to the nearest integer value). In the microcanonical ensemble the total number L of edges is fixed (in contrast to the *canonical* ensemble in which L fluctuates).

As we want to simulate graphs with N up to 10^6 and with an average connectivity α of order $O(1)$, we must use an algorithm which requires computer memory and time of order $O(N)$, not $O(N^2)$. With the microcanonical ensemble, the program is simpler: a random graph is obtained by choosing at random L distinct edges among all the possible edges. From a Monte-Carlo point of view,

the microcanonical ensemble has another advantage: the measurements fluctuate less.

As the graph (or equivalently its adjacency matrix) is very sparse, it is stored in an array T of $2L$ integers, indexed by an array K of $N + 1$ integers; the set of vertices adjacent to the vertex v is the array section $\{T(i)\}$ where $K(v) \leq i < K(v + 1)$. Then the connectivity of v is $K(v + 1) - K(v)$. This defines the array K , with the rules $K(1) = 1$ and $K(N + 1) = 2L + 1$.

Note that each edge $\{v, w\}$ appears twice in T : once for v and once for w . This requires twice more memory than a storage method exploiting the symmetry of the matrix (in which the edges appear only once), but the computational task is faster because the adjacent vertices of a given vertex are simply obtained from arrays T and K .

The leaf removal process is done leaf by leaf. Each time a leaf is removed, the adjacent vertices are examined: if new leaves appear, there are added to a list of potential leaves to be considered later. Each elementary leaf removal requires a computational time of order $O(1)$ and not $O(N)$. So the computational time for the global leaf removal is proportional to the number of removed leaves, which is bounded by $N/2$. Then the total computational time for one random graph (generation and leaf removing) is N times a function of α .

For each random graph, we have measured the number of isolated points $|I|$, the size (number of vertices) of the core N_c , the number of edges of the core L_c and consequently the average connectivity of the core $2L_c/N_c$: there are estimators of $Ni(\alpha)$, $Nc(\alpha)$, $Nl(\alpha)$ and α_{eff} , as defined before. As usual in Monte-Carlo simulations, averages have been done over many random graphs, and their confidence intervals (or error bars) are estimated by the variance of the measurements.

For each value of α , we have generated 10 000 graphs of size $N = 100$, $N = 1000$ and $N = 10 000$, and 1000 graphs of size $N = 100 000$ and $N = 1 000 000$. At the transition value $\alpha = e$, 10 000 graphs have been generated for all the sizes. The whole computation takes a few days on a medium Sun workstation without special optimization.

5.2 Monte-Carlo results

On Fig. 2, Monte-Carlo averages of N_c/N , L_c/N and $2L_c/N_c$ are compared with the infinite N results, $c(\alpha)$, $l(\alpha)$ and α_{eff} . Errors bars are not drawn because they are smaller than the size of symbols. This figure is a typical case of a second order transition. Far from the transition, differences between finite N and thermodynamic (i.e. $N = \infty$) functions are small. Finite size effects are at least of order $1/N$, because the analytical calculations do not take into account the loops of finite size: their number is $O(1)$, so their contributions are $O(1/N)$. The simplest example is the “triangle” subgraph made of three vertices and three edges, not connected to the rest of the graph.

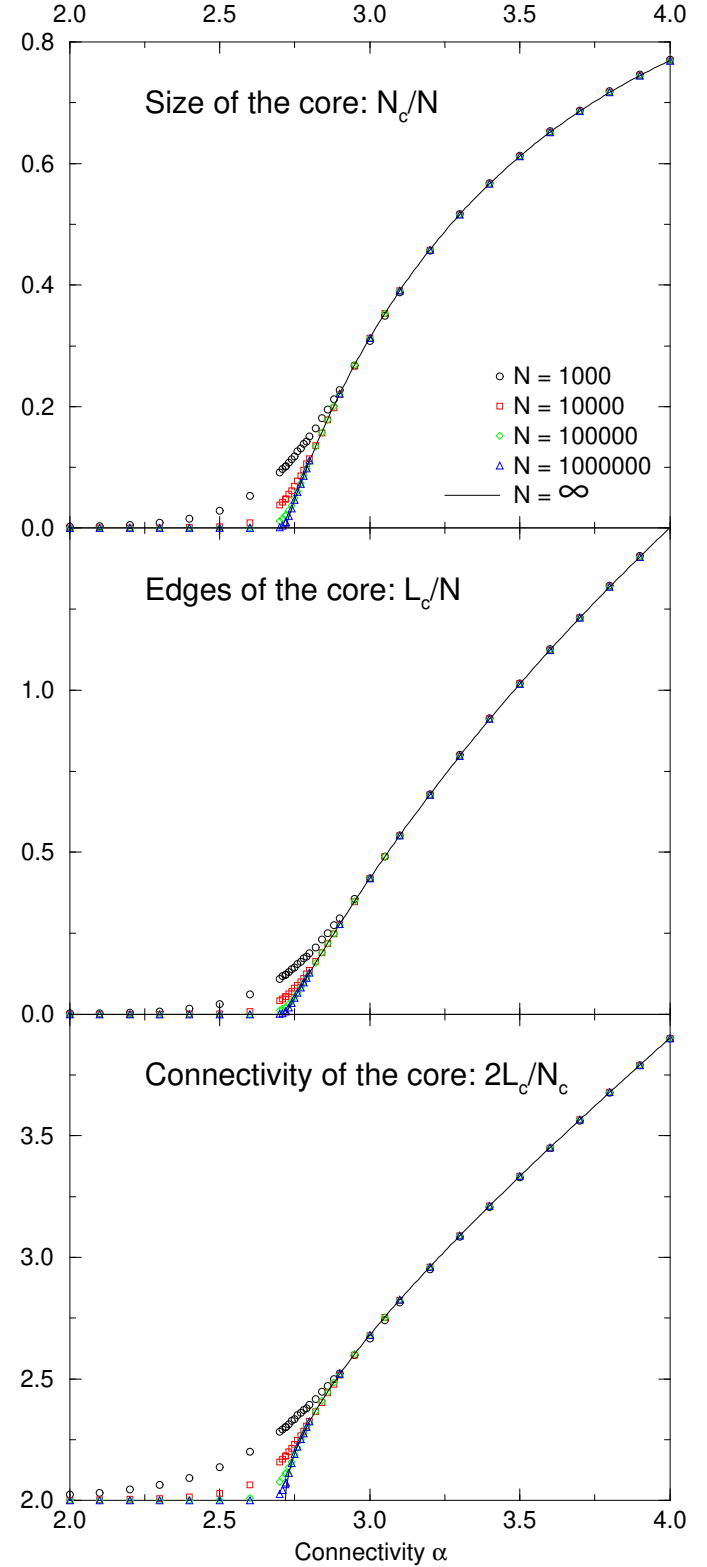


Figure 2: Monte-Carlo averages (symbols) and analytical results (solid line) for the size, edges and average connectivity of the core.

Obviously, the triangles have no leaf and belong to the core: their contribution to N_c is $(\alpha e^{-\alpha})^3/2$.

We have verified that finite size effects are of order $O(1/N)$ (but not larger) for $c(\alpha)$ and $l(\alpha)$ far from the transition. For α_{eff} , this is probably true but less clear because fluctuations are stronger. On the other hand, in the critical region $\alpha \sim e$, finite size effects are larger and some critical exponents can be defined. They are discussed later.

We have also examined the variances of the size, number of edges and average connectivity of the core. For α not too close to e and large N , we expect that the fluctuations (square root of the variance) are of order $O(\sqrt{N})$ for N_c and L_c , and $O(1/\sqrt{N})$ for α_{eff} . So to obtain a large N limit, we define $\chi_c(\alpha) \equiv \text{Var}(N_c)/N$, $\chi_l(\alpha) \equiv \text{Var}(L_c)/N$ and $\chi_\alpha(\alpha) \equiv N \text{Var}(2L_c/N_c)$. These quantities are analogous in the spin models to the magnetic susceptibility (equivalent to the fluctuations of the magnetization).

On Fig. 3, Monte-Carlo estimations of χ_c and χ_l show that $\chi_c(\alpha)$ and $\chi_l(\alpha)$ have a finite limit for $N = \infty$ when $\alpha > e$, a vanishing limit when $\alpha < e$ and diverge when α approaches the critical value e . By analogy with $c(\alpha) \sim l(\alpha) \sim (\alpha - e)$ and $\alpha_{eff} - 2 \sim (\alpha - e)^{1/2}$ when $\alpha \rightarrow e^+$, power laws are expected for the divergences. So, we define two critical exponents ρ and ρ' by

$$\chi_c(\alpha) \sim \chi_l(\alpha) \sim (\alpha - e)^{-\rho}, \quad (5)$$

$$\chi_\alpha(\alpha) \sim (\alpha - e)^{-\rho'}, \quad (6)$$

when $\alpha \rightarrow e^+$. The exponent ρ could be numerically measured by plotting $\log(\chi_c)$ or $\log(\chi_l)$ versus $\log(\alpha - e)$. Unfortunately, this gives poor results because the curvature of the plot is too important, with a slope ρ changing from 1 to 0.5. But it is possible for α_{eff} . Fig. 4 is a log-log plot of $\chi_\alpha(\alpha)$ versus $(\alpha - e)$. Symbols are lined up correctly and the global slope gives the estimation

$$\rho' = 1.5(1).$$

The studies of isolated points are resumed on Fig. 5. Monte-Carlo averages of $|I|/N$ are compared with the infinite N results, $i(\alpha)$: errors bars and finite size effects are so small that they are not visible. On the other hand, the variance $\chi_i(\alpha) = \text{Var}(|I|)/N$ shows bigger statistical fluctuations, but the finite size effects remain small. This variance does not diverge anywhere. However we see a cusp when $\alpha \rightarrow e^+$ compatible with

$$\chi_i(e) - \chi_i(\alpha) \sim (\alpha - e)^\tau$$

with estimations $\chi_i(e) = 0.095(5)$ and $\tau = 0.6(1)$. As $\tau < 1$, the first derivative is infinite at $\alpha = e^+$.

5.3 Finite size scaling

We now concentrate on the finite N behavior, first exactly at the transition $\alpha = e$ and then in the critical region around this transition.

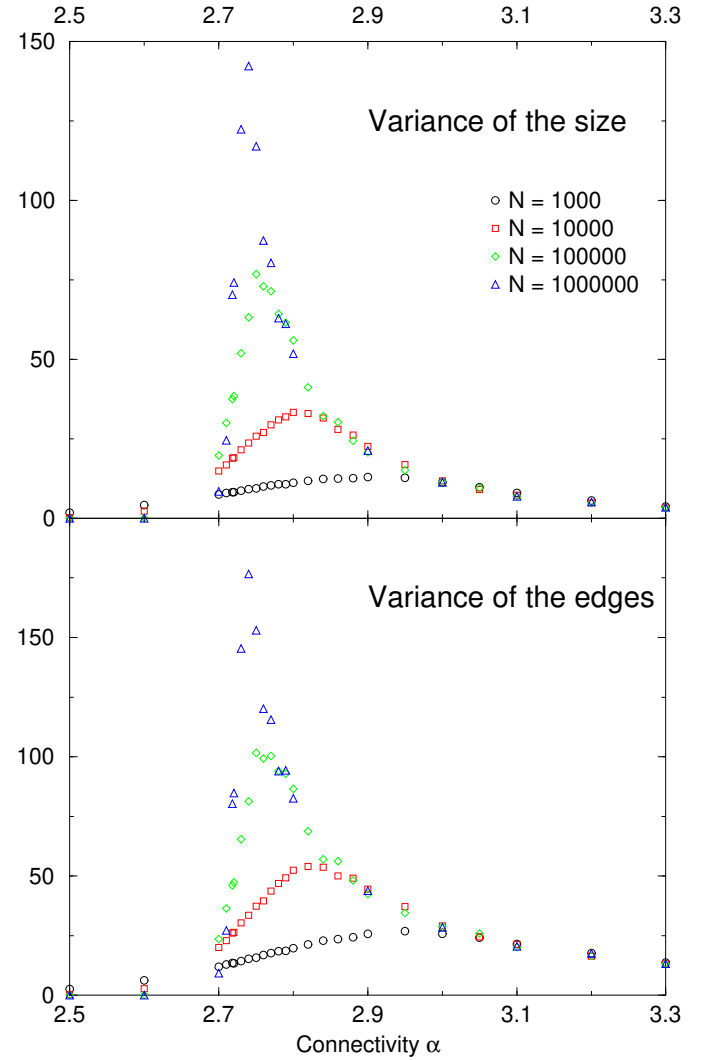


Figure 3: Monte-Carlo estimations of the variance of the size of the core $\chi_c(\alpha)$ and the variance of the number of edges of the core $\chi_l(\alpha)$.

By analogy with the classical percolation transition at $\alpha = 1$ where the size of the largest connected component is [1] of order $O(N^{2/3})$ and its average connectivity is $2 + O(1/N^{2/3})$, we postulate the existence of other critical exponents ω and ϕ defined by

$$N_c \sim L_c \sim N^\omega, \quad (7)$$

$$\alpha_{eff} - 2 \sim N^{-\phi} \quad (8)$$

when $N \rightarrow \infty$ at $\alpha = e$. This hypothesis is tested on Fig. 6: data are correctly fitted by power-laws with

$$\omega = 0.63(1) \text{ and } \phi = 0.21(1).$$

Of course, if the large N behavior is modified by a (power of a) logarithmic function, the true values of the exponents are different than their apparent values when N is large

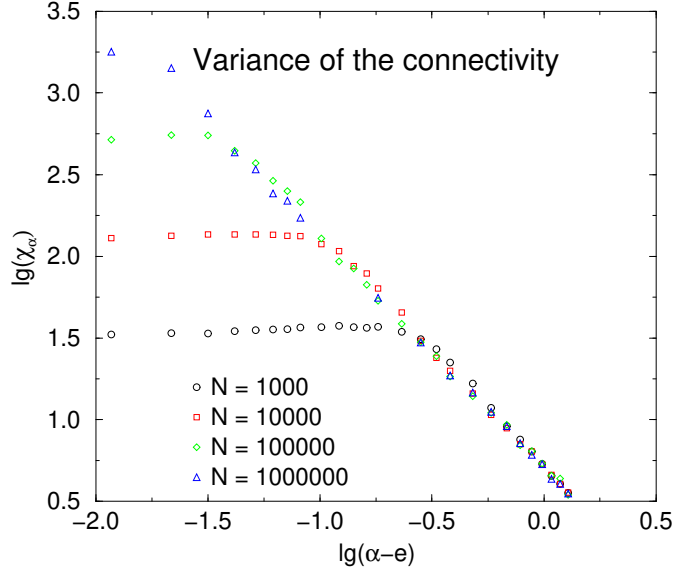


Figure 4: Monte-Carlo estimations of $\chi_\alpha(\alpha)$ (variance of the average connectivity of the core) versus $(\alpha - e)$. The axes are labeled by decimal logarithms.

but finite. Here these exponents are determined by considering the averages of the Monte-Carlo measurements. The width σ of their distributions are also plotted on Fig. 6: means and widths have similar slopes. Consequently

$$\chi_c(e) \sim \chi_l(e) \sim N^{2\omega-1} \quad \text{and} \quad \chi_\alpha(e) \sim N^{1-2\phi} \quad (9)$$

diverge when $N \rightarrow \infty$ at $\alpha = e$.

As widths and means of the Monte-Carlo measurements are of the same order, the distributions remain broad in the large N limit at the transition. On the contrary, when $\alpha \neq e$, the distributions are sharp. On Fig. 7, the cumulative distribution functions $\text{Prob}(N_c/N^\omega \leq x)$, $\text{Prob}(L_c/N^\omega \leq x)$ and $\text{Prob}((2L_c/N_c - 2)N^\phi \leq x)$ are plotted as functions of the scaling variable x for $\alpha = e$. We observe that the curves converge when N is large to scaling distributions (independent of N) and this confirms the hypotheses Eq. (7) and Eq. (8).

When x becomes large, these scaling distribution functions decrease like a Gaussian. Consequently, they are not *large* distributions in the sense that every moment is finite, in agreement with Eq. (9). On the other side, these functions seem to be power laws for small x . This allows to define another exponent δ with

$$\text{Prob}(N_c/N^\omega \leq x) \sim \text{Prob}(L_c/N^\omega \leq x) \sim x^\delta \quad (10)$$

when $x \rightarrow 0$. Our estimation is

$$\delta = 0.36(3).$$

The numerical values suggest that $\omega + \delta = 1$, but we have no argument to explain it.

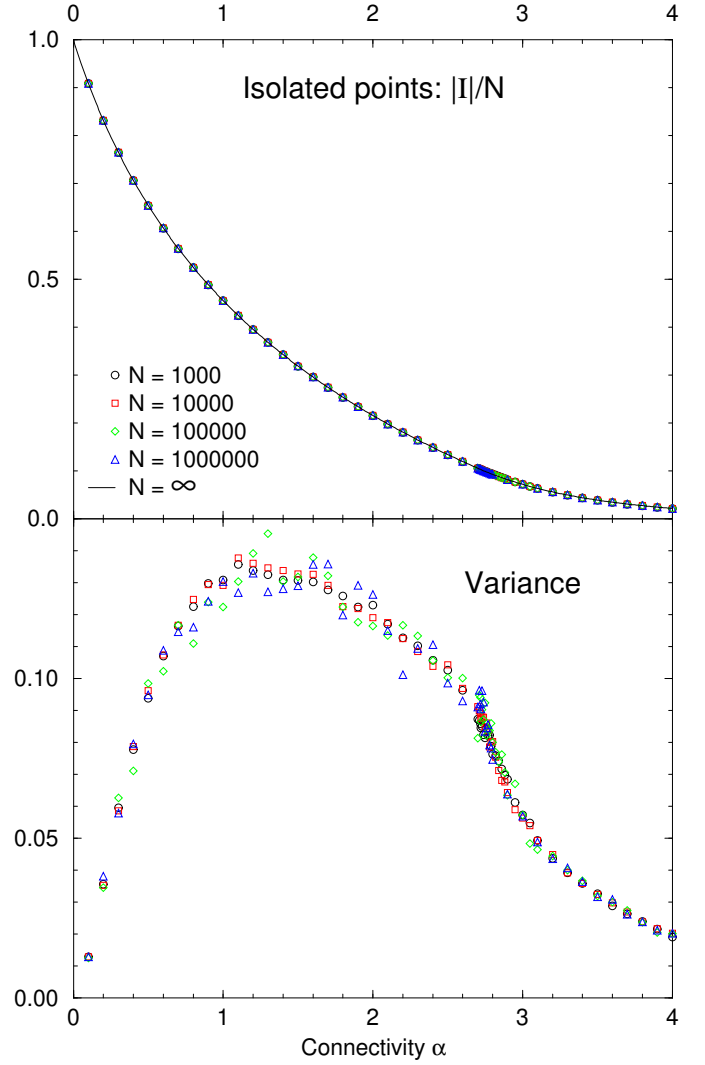


Figure 5: Monte-Carlo averages $|I|/N$ and variance $\chi_i(\alpha)$ of the number of isolated points. The solid line is the analytical result $i(\alpha)$ for $N = \infty$.

By considering the probability that the core of a random graph is void, we measured a new exponent

$$\eta = 0.25(1)$$

where η is defined by

$$\text{Prob}(N_c = 0) \sim N^{-\eta}.$$

The limit $x \rightarrow 0$ in Eq. (10) gives the conjectured relation $\eta = \omega\delta$, which is numerically acceptable. With the hypothesis $\omega + \delta = 1$, it gives $\eta = \omega(1 - \omega)$.

We have also considered $\text{Prob}(L_c = N_c)$, i.e. the probability that the average connectivity of the core is exactly 2. In this case, the core is made of one or several simple loops without branching. The Monte-Carlo study indicates that the large N limit could be a pure number: 0.12(2). More

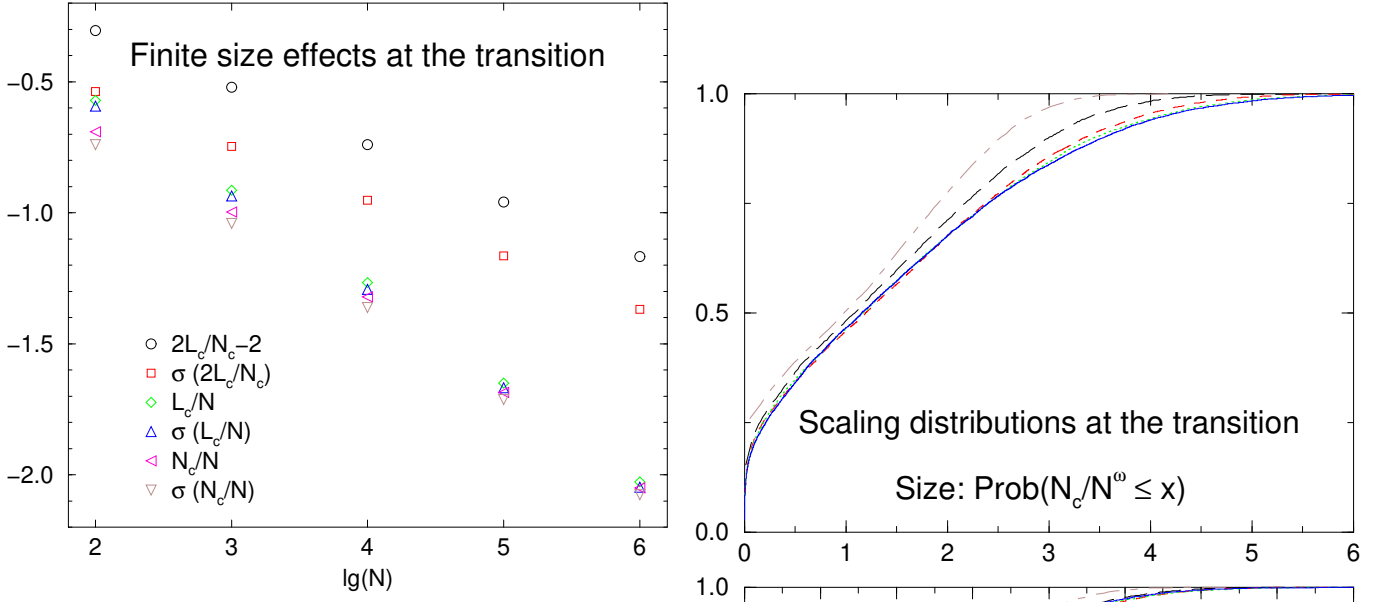


Figure 6: Top to bottom: the average connectivity (mean and width), the number of edges (mean and width) and the size (mean and width) of the core versus the size N of the random graph. The axes are labeled by decimal logarithms. The negative slopes are measurements of $-\phi$ (for the connectivity) and $\omega - 1$ (for size and edges).

intensive simulations are needed to confirm (or invalidate) this result.

More relations between critical exponents can be obtained by using the finite size scaling hypothesis [6]: in the vicinity of the transition, the behavior of finite random graphs is determined by the scaling variable

$$y = (\alpha - e)N^\theta$$

where θ is a positive *scaling exponent*.

First we shortly resume the scaling theory for a general quantity $Q(N, \alpha)$, for size N and connectivity α . For $N = \infty$, let us suppose that

$$Q(\alpha) \sim (\alpha - e)^\gamma$$

when $\alpha \rightarrow e^+$ (γ could be positive or negative). Then we expect in the critical region that

$$Q(N, \alpha) \sim N^{-\gamma\theta} \tilde{Q}(y)$$

where the scaling function $\tilde{Q}(y)$ is defined by

$$\tilde{Q}(y) \equiv \lim_{N \rightarrow \infty} N^{\gamma\theta} Q(N, e + y/N^\theta),$$

which behaves as

$$\tilde{Q}(y) \xrightarrow{y \rightarrow +\infty} y^\gamma.$$

As $y = 0$ exactly at the transition $\alpha = e$,

$$Q(N, e) \sim N^{-\gamma\theta}.$$

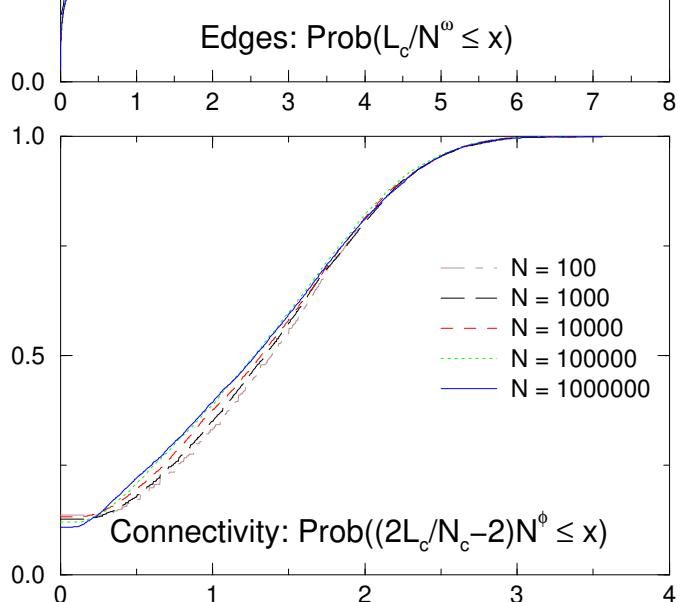


Figure 7: Cumulative distribution functions of the size, the number of edges and the average connectivity of the core, as functions of their respective scaled variables. We have set $\omega = 0.63$ and $\phi = 0.21$.

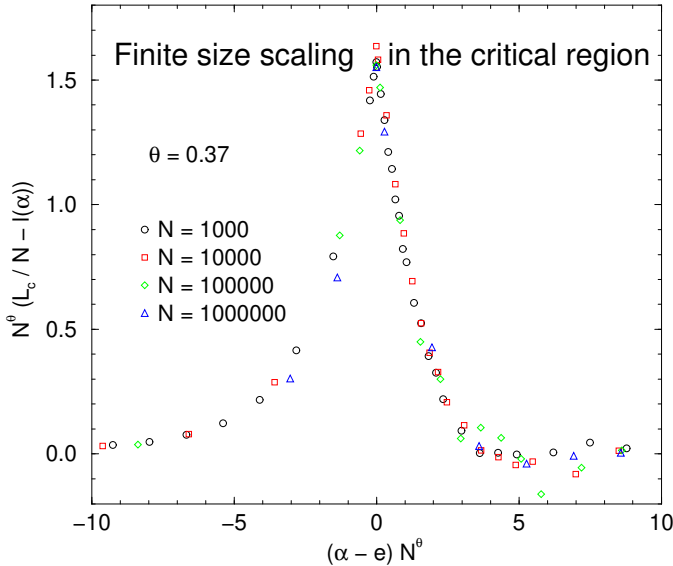


Figure 8: *Finite size scaling for the edges of the core in the critical region.*

So the exponent of finite size effects at the transition and the exponent of critical behavior for $N = \infty$ in the vicinity of the transition are related by θ . This remark is useful only if different quantities share the same θ . For usual models of statistical physics with a 2-D or 3-D geometry (like classical spin systems), the exponent θ describes the divergence of the correlation length ξ . So the uniqueness of ξ implies the uniqueness of θ . Unfortunately for random graphs, we have no equivalent length and no simple phenomenological interpretation for θ . However we shall assume that θ is unique.

As we have computed exact $N = \infty$ formulæ in Sect. 4, we can directly study $Q(N, \alpha) - Q(\alpha)$, i.e. the finite size effects. The scaling function is now $\tilde{Q}(y) - y^\gamma$ and is maximal around $y = 0$. From a numerical point of view, the analysis becomes easier than the one of the monotonic function $\tilde{Q}(y)$.

Let us now consider N_c/N and L_c/N . As $c(\alpha) \sim l(\alpha) \sim (\alpha - e)$ when $\alpha \rightarrow e^+$, for these quantities $\gamma = 1$. Then

$$\theta = 1 - \omega.$$

On Fig. 8, with the choice $\theta = 0.37$ (induced by the numerical measure of ω), $N^\theta(L_c/N - l(\alpha))$ is plotted versus $y = (\alpha - e)N^\theta$. We see that data are well superposed: they draw the scaling function. Note that θ is the unique fitting parameter for this figure.

Let us now consider the variances $\chi_c(\alpha)$ and $\chi_l(\alpha)$. Using Eq. (5) and Eq. (9), the finite size scaling hypothesis gives the new relation

$$\rho\theta = 2\omega - 1.$$

The same analysis with the average connectivity of the core can be done. As $\alpha_{eff} - 2 \sim (\alpha - e)^{1/2}$, the cor-

	θ, δ	ω	ϕ	ρ	ρ'	η
MC	0.36(3)	0.63(1)	0.21(1)		1.5(1)	0.25(1)
a	1/3	2/3	1/6	1	2	2/9
b	0.37	0.63	0.185	0.70	1.70	0.233
c	2/5	3/5	1/5	1/2	3/2	24/100
d	0.42	0.58	0.21	0.38	1.38	0.244

Table 1: *Critical exponents for the geometric phase transition when the average connectivity of a large random graph is $\alpha = e$. The line “MC” displays the results of Monte-Carlo simulations. The lines “a-d” are a few sets of values compatible with scaling relations. The line “c” has our preference (see text).*

responding $\gamma = 1/2$. Using Eq. (8), the scaling relation is

$$\theta = 2\phi.$$

For the variance of the connectivity χ_α , Eq. (6) and Eq. (9) give

$$\rho'\theta = 1 - 2\phi.$$

By eliminating θ , other relations are obtained: $\rho' = \rho + 1$ and $2\phi + \omega = 1$.

With these four scaling relations and the Monte-Carlo determinations, we will now try to conjecture the *exact* values of these exponents. Table 1 resumes the following considerations. The results of Monte-Carlo simulations are given in line “MC”. Other lines are suggestions for sets of exponents compatible with the four scaling relations.

The line “b” is obtained by using the numerical determination of ω and the scaling relations. In particular, it gives $\theta = 0.37(1)$. The line “d” uses the numerical determination of ϕ ; it gives $\theta = 0.42(2)$. As the difference between these two values of θ is about twice larger than the uncertainty, we cannot definitely conclude whether the size and the connectivity of the core share the same scaling exponent θ or not.

The line “a” is obtained by assuming that $\omega = 2/3$ and $\theta = 1/3$, which are the values [1] of the corresponding exponents for the classical percolation of random graphs at $\alpha = 1$. This hypothesis seems incompatible with the Monte-Carlo estimations of ϕ and ρ' . Furthermore the average connectivity of the giant component near the classical percolation transition behaves with $2 + O((\alpha - 1)^2)$ — to be compared with $2 + O((\alpha - e)^{1/2})$ for the core — and consequently the corresponding exponent ϕ is $2\theta = 2/3$ (but not $\theta/2 = 1/6$). So in any case, the analogy between exponents of percolation and core transitions cannot be complete.

The line “c” assumes that the exponent $\rho' = 1.5(1)$ is exactly $3/2$. This is very attractive because exponents are simple rational fractions and the value $\theta = 2/5$ is between the numerical estimations 0.42 and 0.37.

Of course, nothing in the theory of critical phenomena requires that critical exponent are rational numbers with

small numerators (for a recent example, see Ref [7]). However, if we want conciliate numerical simulations, theoretical considerations and simple rational fractions, we are led to conjecture $\omega = 3/5$, $\phi = 1/5$, $\rho = 1/2$, $\rho' = 3/2$, $\delta = \theta = 2/5$ and $\eta = 6/25$.

To reduce the uncertainties in Monte-Carlo simulations, bigger size N are needed, in particular in the case where the large N behavior would be affected by logarithmic law. We hope to progress in analytical methods for calculating these exponents as well.

6 Applications

We now discuss two applications of our results on the core: the first one to the conductor-insulator transitions in random graphs and the second one to combinatorial optimization problems.

6.1 Localization on random graphs

We denote by $Z(G)$ the dimension of the kernel (the subspace of eigenvectors with eigenvalue 0) of the adjacency matrix of the graph G . It is known [8] that $Z(G)$ is invariant under leaf removal (see Ref. [9] for a proof and an application to random trees). As the adjacency matrix is block-diagonal with one block per connected component, $Z(G)$ is additive on connected components. These two properties imply that

$$Z(G) = Z(C) + Z(I) = Z(C) + |I| \leq N_c + |I|.$$

The last equality is because the adjacency matrix vanishes for a collection of isolated points.

Taking the average of these formulæ for random graphs and using our results on the core, we get that $Z(G) = Nz(\alpha) + o(N)$ for a large random graph G with average connectivity α , with

$$\begin{aligned} z(\alpha) &= i(\alpha) \quad \text{for } \alpha \leq e, \\ i(\alpha) &\leq z(\alpha) \leq c(\alpha) + i(\alpha) \quad \text{for } \alpha > e. \end{aligned} \quad (11)$$

It has been argued in Ref. [4] that

$$z(\alpha) = \frac{A + B + AB}{\alpha} - 1 \quad (12)$$

for all values of α . Combined with our present results, this means that

$$z(\alpha) = i(\alpha) \quad \text{for all values of } \alpha.$$

We may interpret Eq. (11) as an independent proof of Eq. (12) for $\alpha \leq e$ and we may also infer that the adjacency matrix of the core of a random graph at $\alpha > e$ has a kernel of size $o(N)$.

In Ref. [4], it was shown that e is in a domain of the α parameter for which delocalized vectors are responsible

for a finite fraction of the size of the kernel. Imagine that we start to increase α very slowly from $\alpha = e$ by adding randomly new edges one by one to the random graph. We watch the competition between the core (which, we have seen, carries few elements in the kernel), the localized eigenvectors in the kernel and the delocalized ones. The competition between the core and the full kernel is not very strong: when n edges, with $1 \ll n \ll N$, are added to the graph, the core grows in average of $24 e^{-2}n$ vertices, while $e^{-2}n$ vectors in the kernel are lost. However, by the results of Ref. [4], about n^2 delocalized eigenvectors disappear and n^2 localized eigenvectors replace these. It is intuitive that delocalized eigenvectors in the kernel, which live on large structures on the random graph, have a high probability to be perturbed by the growing core. But the precise mechanism by which their extinction is almost compensated by new localized vectors in the kernel remains to be elucidated.

The concept of leaf removal process can also be used to analyze the localization-delocalization transitions that occur at $\alpha_d \approx 1.42153$ and $\alpha_r \approx 3.15499$. As shown in Ref. [4], the localized eigenvectors in the kernel live on definite structures that can be drawn on the random graph. These structures are finite (connected) trees that

- can be bicolored brown-green in such a way that all vertices with 0 or 1 neighbor are green and all neighbors of the green vertices in the random graph belong to the tree; the neighbors of the brown vertices on the other hand, can be anywhere on the random graph.
- are maximal, i.e. are not part of a larger tree with the same properties. Observe that each isolated point is maximal.

We can put marks on all vertices belonging to such structures and build histories of leaf removal processes such that the initial steps remove only marked vertices, and after these steps, the only remaining marked vertices are now isolated.

Then if α is small ($\alpha \leq \alpha_d$) or large ($\alpha \geq \alpha_r$), the number of isolated marked points is $Ni(\alpha) + o(N)$. This implies in particular that at most $o(N)$ bunches of the the remaining graph contain more than one leaf.

On the other hand, if $\alpha \in [\alpha_d, \alpha_r]$ the number of isolated marked points is less than $Ni(\alpha)$: a number of order N of non-trivial bunches will have to appear somewhere during the rest of the leaf removal process.

6.2 Vertex covers and cousins

Apart from the size of the kernel, several other interesting quantities attached to graphs behave rather simply under leaf removal. We mention two, which are related to combinatorial optimization problems.

Vertex cover: A vertex cover of a graph is a subset of the vertices containing at least one extremity of every

edge of the graph. We denote by $X(G)$ the minimal size of a vertex cover of a graph G .

Edge disjoint subset: An edge disjoint subset is a subset of the edges such that no two edges in the subset have a vertex in common. We denote by $Y(G)$ the maximal size of edge disjoint subset in a graph G .

There is a nice “practical” interpretation of $X(G)$. Imagine that the edges of the graph are the (linear) corridors of a museum, the vertices corresponding to ends of corridors. A guard sitting at a vertex can control all the incident corridors. So $X(G)$ is the minimum number of guards needed to control all corridors of the museum.

A similar interpretation of $Y(G)$ is possible, but anyway, the determination of $X(G)$ or $Y(G)$ for a given G is archetypal of a class of difficult optimization problems of interest for theoretical computer science for instance. They are called Non-deterministic Polynomial (NP) because no polynomial time algorithm is known to solve them (and such an algorithm is not expected to exist, this is related to the famous $P \neq NP$ conjecture), but given a candidate solution, it is easy to check in polynomial time that it is correct.

When G is a random graph, ideas from physics can be applied, using for instance techniques first introduced to study spin-glasses. For fixed α , let $x(\alpha)$ and $y(\alpha)$ denote the limits of the averages of $X(G)/N$ and $Y(G)/N$ when G is a random graph of size N and $N \rightarrow \infty$. The replica trick has been used by Hartmann and Weigt in a series of papers [3, 10, 11]. They have shown that for $\alpha \leq e$, the replica symmetric solution is stable, whereas it becomes unstable for $\alpha > e$. The replica symmetric solution leads to

$$x(\alpha) = 1 - \frac{2W + W^2}{2\alpha} \quad \text{for } \alpha \leq e.$$

This relation has to break down somewhere, because a result of Frieze [12] implies that

$$x(\alpha) = 1 - \frac{2}{\alpha}(\log \alpha - \log \log \alpha - \log 2 + 1) + o\left(\frac{1}{\alpha}\right),$$

whereas $W \sim \log \alpha$ for large α , so that the asymptotics of $1 - \frac{2W + W^2}{2\alpha}$ starts with $1 - \frac{\log^2 \alpha}{2\alpha}$. Weigt and Hartmann [11] have also used a good algorithm to get an approximation of a minimal vertex cover. The idea is essentially to look for a vertex with a maximal number of incident corridors and put a guard there. Then remove the site and the adjacent corridors and iterate. This is always fast, but gives only an upper bound for $X(G)$. This can be refined, but then the algorithm needs a very long time when $\alpha > e$.

We show how leaf removal can be applied to the museum guard problem. If (v, w) is a leaf of G , there is a minimal vertex cover with a guard at v . This is because any vertex cover has a guard at v or at w , and a guard at v makes the guard at w useless. So if a minimal vertex cover has a guard at w , moving it to v yields another minimal vertex cover. Isolated vertices do not need guards.

The leaf removal of (v, w) leading from G to G' removes exactly the corridors controlled by the guard at v . Hence $X(G) = X(G') + 1$.

An analogous argument applies to maximum edge disjoint subsets. Indeed, if (v, w) is a leaf of G , there is a maximal edge disjoint subset that contains $\{v, w\}$. This is because if no edge of an edge disjoint subset touches v , this edge disjoint subset is not maximal (it can be completed with $\{v, w\}$), and if an edge disjoint subset has an edge that touches v , replacing this edge by $\{v, w\}$ yields an edge disjoint subset of the same size. The leaf removal of (v, w) leading from G to G' removes, apart from $\{v, w\}$, exactly the edges that cannot belong to any edge disjoint subset containing $\{v, w\}$. Hence $Y(G) = Y(G') + 1$.

Some general inequalities can be proved. For instance $X(G) \geq Y(G)$ (the triangle is an example when the inequality is strict) and $Z(G) \geq N - 2X(G)$. However, $Z(G) - N + 2Y(G)$ can have any sign (negative for the triangle but positive for the square).

Anyway, at each leaf removal, two vertices are removed, so $Z(G)$, $N(G) - 2X(G)$ and $N(G) - 2Y(G)$ are invariant under leaf removal. Moreover, X and Y vanish for unions of isolated vertices. To summarize, we have shown that

$$\begin{aligned} X(G) &= X(C) + \frac{N - N_c - |I|}{2} \\ Y(G) &= Y(C) + \frac{N - N_c - |I|}{2} \\ Z(G) &= Z(C) + |I|. \end{aligned}$$

When G is a random graph with $\alpha < e$, the core is small ($o(N)$ for large N). Thus,

$$x(\alpha) = y(\alpha) = \frac{1 - z(\alpha)}{2} = 1 - \frac{2W + W^2}{2\alpha} \text{ for } \alpha \leq e,$$

which gives in particular an independent proof of the result of Weigt and Hartmann [3]. Note that in this case, the approximate algorithm is to put a guard at a vertex touching as many edges as possible, then remove it and iterate, whereas the exact algorithm is almost the opposite, namely, put a guard at the connected end of a leaf, remove the leaf and iterate. Leaf removal gives a very fast algorithm (linear in N if the graph is properly encoded) to construct a minimal vertex cover when $\alpha < e$.

If $\alpha > e$, leaf removal stops while an extensive number of edges is still present: this gives a lower bound which is very poor at large α . But it seems clear that the replica symmetry breaking [11] at $\alpha = e$ is closely related to the fact that the structure of the core of a random graph is more complicated than the structure of the parts eliminated by leaf removal, so that a more refined Parisi order parameter is needed to describe the phase $\alpha > e$.

7 Conclusions

In this paper we have unraveled the nature of a new geometric second order phase transition in random graphs and shown the emergence of a core at threshold $\alpha = e$. This core is the residue when leaves and isolated points are iteratively removed. We have argued that the core is dominated by a giant component. The dominant contribution of the large N behavior of the relevant thermodynamical quantities was computed exactly. We have studied numerically the finite size behavior of the core, defined a variety of new critical exponents and obtained approximations consistent with their mutual relationships. Finally, we have applied our results to the localization transition and to combinatorial optimization problems on random graphs.

However, some more analytical or numerical work is needed to identify without any doubt the exponents for the phase transition at $\alpha = e$. An open question is the interaction between the emergence of the core and the delocalized eigenvectors of the adjacent matrix with eigenvalue 0. A fine study of the distribution of the sizes of the connected components of the core could be done with Monte-Carlo simulations: for $\alpha > e$, we expect a giant component, plus a finite number of finite components. Moreover we have shown that the number of eigenvectors with eigenvalue 0 living on the core is $o(N)$ and numerical simulations could give the precise asymptotics.

Finally, as the core percolation appears in a simple model of random graphs, which is governed only by one parameter, the average connectivity α , we expect that this transition is *universal* in the sense that some characteristics of this transition (second order, critical exponents, etc., but not the precise value of $\alpha = e$ at the transition) could be seen in other models or real materials.

References

- [1] P. Erdős and A. Rényi, *On the evolution of random graphs*, Publ. Math. Inst. Hungar. Acad. Sci. 5 (1960) 17–61.
- [2] S. Janson, D.E. Knuth, T. Luczak and B. Pittel, *The birth of the giant component*, Random Structures and Algorithms 4 (1993), 233–358.
- [3] M. Weigt and A.K. Hartmann, *Number of guards needed by a museum: a phase transition in vertex covering of random graphs*, Phys. Rev. Lett. 84 (2000) 6118, [arXiv:cond-mat/0001137](https://arxiv.org/abs/cond-mat/0001137).
- [4] M. Bauer and O. Golinelli, *An exactly solvable model with two conductor-insulator transitions driven by impurities*, to be published in Phys. Rev. Lett. (2001), [arXiv:cond-mat/0006472](https://arxiv.org/abs/cond-mat/0006472).
- [5] M. Bauer and O. Golinelli, *Random incidence matrices : moments of the spectral density*, to appear in J. Stat. Phys., [arXiv:cond-mat/0007127](https://arxiv.org/abs/cond-mat/0007127).
- [6] For a general presentation, see M. N. Barber, *Finite-size scaling*, in Vol. 8 of *Phase transitions and critical phenomena*, edited by C. Domb and J. L. Lebowitz (Academic Press 1983).
- [7] P. Di Francesco, O. Golinelli, E. Guitter, *Meanders: exact asymptotics*, Nucl. Phys. B 570 (2000) 699–712, [arXiv:cond-mat/9910453](https://arxiv.org/abs/cond-mat/9910453).
- [8] D.-M. Cvetković, M. Doob and H. Sachs, *Spectra of Graphs*, Academic Press, New York, 1980.
- [9] M. Bauer and O. Golinelli, *On the kernel of tree incidence matrices*, J. Integer Sequences, Article 00.1.4, Vol. 3 (2000), <http://www.research.att.com/~njas/sequences/JIS>.
- [10] A.K. Hartmann and M. Weigt, *Statistical mechanics perspective on the phase transition in vertex covering of finite connectivity random graphs*, [arXiv:cond-mat/0006316](https://arxiv.org/abs/cond-mat/0006316).
- [11] M. Weigt and A.K. Hartmann, *Minimal vertex covers on finite-connectivity random graphs — a hard-sphere lattice-gas picture*, [arXiv:cond-mat/0011446](https://arxiv.org/abs/cond-mat/0011446).
- [12] A.M. Frieze, *On the independence number of random graphs*, Discr. Math. 81 (1990) 171.